STUDIA UBB PHYSICA, Vol. 61 (LXI), 2, 2016, pp. 7-20
(RECOMMENDED CITATION)

Dedicated to Professor Dr. Sorin Dan Anghel on His 65th Anniversary

EXCITED STATE PROPERTIES OF THE CAMPHORQUINONE PHOTOINITIATOR

M. ABDALLA[a], LARISA MILENA ŢIMBOLMAŞ[a], N. LEOPOLD[a], SANDA CÎMPEAN[b], V. CHIŞ[a*]

ABSTRACT. The photophysics of the photoinitiator Camphorquinone was investigated computationally in this work, by using time-dependent Density Functional Theory methods. DFT calculations. We fully assigned the UV-Vis electronic transition of the Camphorquinone monomer. Moreover, the emission energy as well as the structural differences between the geometries of the molecule in the ground and excited state have been analyzed.

Keywords: *Camphorquinone; photo-initiator; excited state; TD-DFT*

1. INTRODUCTION

The commonly used resin based composites (RBCs) in dentistry are based on poly methyl methacrylates filled with particles whose role is to give strength, wear resistance and the reduction of the polymerization shrinkage [1, 2]. Basically, a dental composite contains a resin based matrix, fillers and coupling agents. The resin based matrix (Fig.1) consists of monomers (e.g., Bisphenol A-glycidyl methacrylate (Bis-GMA), Urethane dimethacrylate (UDMA)), low viscosity co-monomers like Triethylene glycol dimethacrylate (TEGDMA), initiators, co-initiators, inhibitors and pigments.

[a] *Babeş-Bolyai University, Faculty of Physics, 1 Kogălniceanu, Cluj-Napoca, Romania*
[b] *Department of Conservative Dentistry and Endodontics, Faculty of Dental Medicine, Iuliu Hatieganu University of Medicine and Pharmacy, 33 Motilor, Cluj-Napoca, Romania*
[*] *Corresponding author: vasile.chis@phys.ubbcluj.ro*

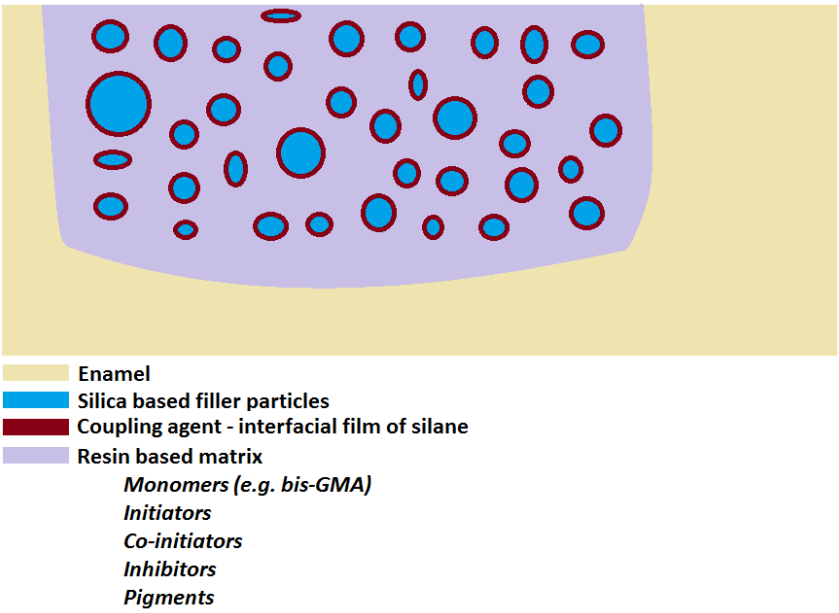

Fig. 1. Ingredients of the composite materials used in dentistry

Polymerization Initiators (photosensitizer) for new composites are chemical compounds able to absorb light and to initiate the polymerization process. Even though there are three primary absorbers in the composite (the initiator, the monomer/co-monomer resin and the pigment added to achieve the correct tooth shade) only the light absorbed by the initiator will be used in the photo-curing process [3].

One of the most used initiator in the commercially available composites is Camphorquinone (CQ, Fig.2), for which the absorption range corresponds to visible light wavelength between 400-500 nm, with λ_{max} at about 470 nm. CQ abstracts a hydrogen atom from the tertiary amine added as co-initiator, resulting in free-radical generation. Obviously, the optimum efficiency is obtained when the absorption peak of the photoinitiator is in resonance with the spectral emission from the light curing unit.

Polymerization co-initiator is a chemical compound that interacts with the activated camphorquinone to produce reactive species able to initiate and sustain the polymerization process. The type of co-initiator as well as the photoinitiator/ coinitiator ratio can affect drastically the degree of conversion, polymerization rate or the biocompatibility of the materials [4].

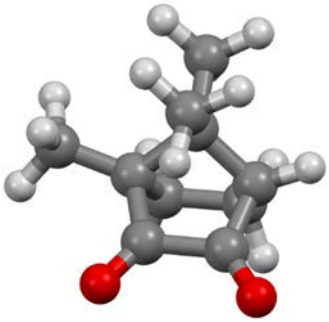

Fig. 2. Optimized molecular structure of Camphorquinone at B3LYP/6-311+g(2d,p) level of theory

Tertiary amines are commonly used as co-initiators in the resin-based composites. Examples of such amines used in the photoactivated composites are basically Dimethylaminoethylmetacrylate (DMAEMA) and Ethyl-4-dimethylamino-benzoate (EDMAB, see Fig. 3).

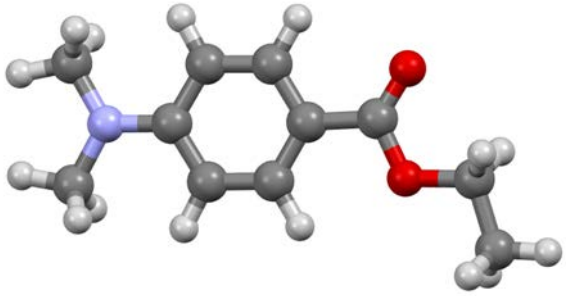

Fig. 3. Optimized molecular structure of EDMAB at B3LYP/6-311+g(2d,p) level of theory

In this work, we aimed to shed more light on the excited state of camphorquinone photoinitiator. For this purpose we calculated both, the absorption and emission energies for this compound and compared the computational data to the reported experimental results [5, 6]. Also, an analysis of the electronic transitions is included here, as well as the geometry of the molecule in its first excited state.

2. COMPUTATIONAL DETAILS

Absorption spectrum and the geometry of the CQ in the first excited state was calculated using the time-dependent DFT (TD-DFT) methodology [7], implemented in the Gaussian09 package [8]. For these purposes we used the B3LYP functional [9-12], coupled with the 6-311+g(2d,p) basis set.

The simulated UV-vis spectrum of CQ in the 140–500 nm range has been obtained by summation of the contributions from transitions to the first 30 singlet excited electronic states. The UV spectral line-shapes were convoluted with Gaussian functions with FWHM of 0.44 eV.

The nature of the excited states has been analyzed using the Natural Transition Orbitals (NTO) formalism proposed by Martin [13], that offers compact description of the electronic excitations with the advantage that only one or two occupied/virtual pairs of orbitals are enough for a clear interpretation of the physical nature of the excited states involved in absorption and emission processes [14].

The solvent effects have been considered by using the implicit Polarizable Continuum Model (PCM) [15].

All the calculations have been performed with the Gaussian Rev E.01 [8] software package and the results have been analyzed using the GaussView program [16].

Figures representing the structures of CQ were have been created using the Mercury 3.3 [17] software package.

3. RESULTS AND DISCUSSIONS

3.1 Absorption spectrum of Camphorquinone

Camphorquinone (CQ) is widely used as a type II photoinitiator for the photocuring of restorative dental composite resins [18, 19]. The excitation energy of the photoinitiator must be in resonance with the energy of the photons emitted by the lamps or LEDs used for curing. Moreover, another important requirement is to have no competing absorptions by the components of the composites at the excitation energy of the photoinitiator. Thus, from practical applications, information about the photoinitiator absorption spectrum is essential [20 Neu05]. From fundamental perspective, of great importance is also the geometry change of the photoinitiator as a result of electronic excitation.

The UV-Vis spectra of CQ were reported recently by Longhi et al. [5] in ethanol, Okulus et al. in chloroform and in methanol [6]. The experimental spectra show a weak transition around 470 nm, with a slight influence of the solvent.

Fig. 4 illustrates the calculated absorption spectrum of CQ in acetonitrile, at PCM-B3LYP/6-311+G(2d,p) level of theory. The most intense electronic transitions for this compound occur in the UV range. A weak transition is calculated at 484 nm, in the visible range and this corresponds to the λ_{max} of CQ and it is correlated to the activating energy of the photoinitiator. Both, the band position and molar absorptivity for this transition are in excellent agreement with the experimental data.

Acetonitrile was used as solvent because of its polar aprotic nature (dipole moment: 3.92D), and consequently it will hardly be involved in intermolecular hydrogen bonds with the CQ monomers. For comparison purposes, ethanol was also used as implicit solvent but no significant difference was observed in the calculated UV-Vis spectrum compared to acetonitrile.

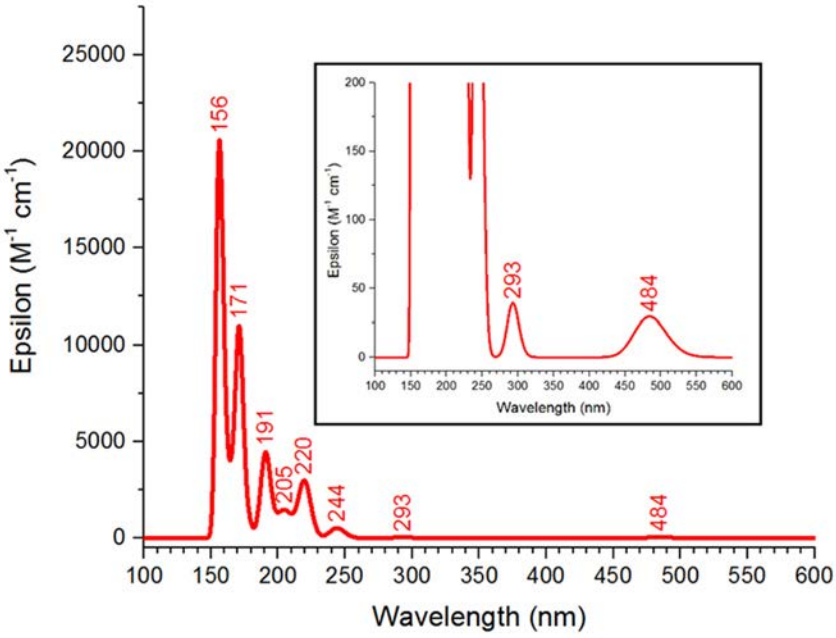

Fig. 4. B3LYP/6-311+g(2d,p) calculated absorption spectrum of camphorquinone in acetonitrile (PCM was used as solvent model; inset: zoom in the low-values region of the molar absorptivity)

All the calculated excitation energies of the CQ monomer in acetonitrile are listed in Table 1. To better understand the properties of the excited states of CQ we obtained the NTOs based on the calculated density matrices.

As seen in Fig. 4 and Table 1, the most intense transitions appear at wavelengths between 130 and 260 nm and they are due to transitions to S26, S19, S11, S5 and S3 excited states. S3, S5 and S11 excited states involve the frontier orbitals HOMO and LUMO as final or initial state of transition, while the S19 and S26 states imply transition between either low lying occupied orbitals like HOMO-10, HOMO-12 and HOMO-14 or to high unoccupied orbitals like LUMO9. On the other hand, the transition corresponding to the excitation to the S2 state is predicted at 272 nm and it is due to the HOMO-1-> LUMO and HOMO-2-> LUMO transitions with 63 % and 13 % contributions, respectively.

The state of interest for CQ as a photoinitiator is S1, with the calculated λ = 484 nm, resulted as a 97 % HOMO-LUMO transition. As seen in Fig. 4, this transition, but also the transition to the S2 state is characterized by a much lower molar absorptivity than the excitations calculated at lower wavelengths.

Table 1. Theoretical UV-Vis absorption spectral data calculated for the CQ monomer and in acetonitrile at PCM-B3LYP/6-311+G(2d,p) level of theory

Excited state	**λ(nm)**	**f[a)]**	**transitions[b)]**	**Contributions (%)[c)]**
S1	446.0	0.0003	H→L	97
S2	272.0	0.0002	H-1→L H-2→L	63 13
S3	214	0.0084	H-2→L H-3→L	60 29
S5	190	0.0265	H-3→L	65
S11	172	0.0484	H→L+2	60
S19	151	0.0285	H-10→L H-1→L+9	12 11
S26	142	0.0972	H-14→L	45
			H-12→L	8

[a)] only those transitions corresponding to the bands reported in Fig. 3.2.1.1 are included
[b)] H – HOMO and L – LUMO
[c)] only the first two major contributions are included

Thus, the calculated ε values for S1 and S2 transitions (29.6 and 19.9 $M^{-1}cm^{-1}$, respectively) is about three order of magnitudes lower than those corresponding to the higher energy transitions (23287 $M^{-1}cm^{-1}$ for the S26 state). The experimental ε value reported for S1 transition of CQ in ethanol [21] is 28 $M^{-1}cm^{-1}$ and the experimentally reported λ_{max} for CQ are: 470 nm in chloroform [6] and ethanol [21] and 472 nm in toluene [22].

Commonly, in order to describe a particular transition to an excited state one uses the molecular orbitals. However, for some transitions there can exist more contributions to that particular transitions, making very difficult the analysis of based on the frontier MOs. An alternative is to use the natural transition orbitals (NTOs) which are a transformed version of the canonical orbitals and can be calculated on the basis of the transition densities [23]. This formalism offers compact description of the electronic excitations with the advantage that only one or two occupied/virtual pairs of orbitals are enough for a clear interpretation of the physical nature of the excited states involved in absorption and emission processes. The advantage of using NTOs is that a particular transition can be described by using a single pair of such orbitals – one occupied and one unoccupied.

It is a common practice to denote the occupied NTOs as “hole transition orbitals” and the unoccupied NTOs as “particle transition orbitals” [24, 25]. Fig. 5 illustrates the NTOs for the main electronic transitions of CQ monomer in acetonitrile.

Quantum chemical calculations give a clear picture of the emergence of electronic transition to S1 state. Thus, as observed in Fig. 5, both, the hole and particle NTOs are delocalized onto the ketone groups of CQ. Moreover, the particular shapes of the two NTOs suggest a n -> π^* transition, that is, an electronic transition described as promotion of an electron from a non-bonding (lone-pair) orbital localized on the oxygen atoms of CQ to the antibonding π^* orbital, also localized mainly on the two oxygen atoms.

3.2. Emission energy and fluorescence lifetime of Camphorquinone

The excitation energy and the identity of the molecular orbitals involved are only a part of the parameters used to describe the molecular excited states. Other important parameters of the excited states are the (vertical) emission energy and fluorescence lifetime. Both of them are very sensitive to the molecular conformation or to the environment of the chromophore. While the emission energy can be routinely measured, obtaining the experimental values of the fluorescence lifetime is much more challenging but it still can be done by using time-resolved fluorescence technique.

From computational point of view, the calculation of these parameters imply geometry optimization of the molecule in a particular excited state. Nowadays, such calculations can be done using high performance computers.

Figure 6 summarizes the points on the ground and excites potential energy surface that need to be calculated for obtaining the emission energy.

Particularly, for estimating the vertical emission energy we need the energy minimum on the potential surface of the excited state and the energy calculated on the geometry of the excited state. The difference between the two values gives the vertical emission energy.

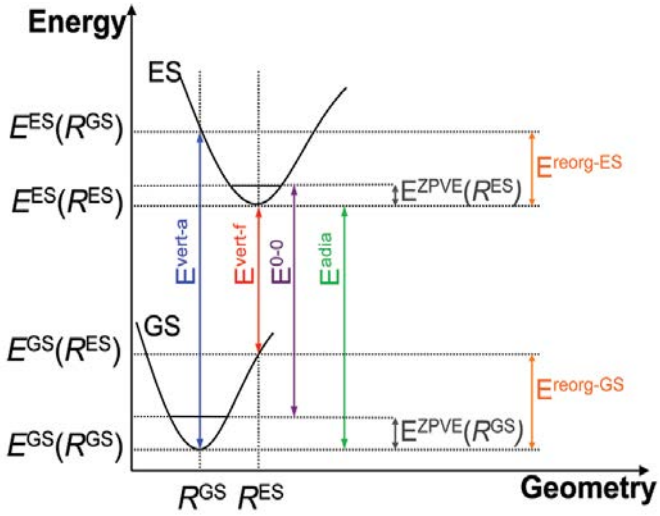

Fig. 6. Ground and excited states energies necessary to be computed for obtaining the emission energy of a molecules

Based on the model of vertical transitions, the radiative emission rate k_r can be obtained by [26]:

$$k_r = \frac{4}{3}\frac{\Delta E^3}{c^3}\mu_{10}^2$$

where c is the speed of light, , ΔE is the energy of the S1 → S0 transition and μ_{10} is the dipole strength. ΔE and μ_{10} must be evaluated at the energetic minimum corresponding to the excited state [27].

Having obtained k_r, the radiative fluorescence lifetime is calculated as $\tau_r = 1/ k_r$.

Table 2 summarizes the calculate parameters necessary for the estimation of the vertical emission energy and the radiative fluorescence lifetime.

We have to mention that no experimental result was reported in the literature related to the fluorescence lifetime of CQ. Our estimation for the radiative part of the fluorescence lifetime is very large compared to other molecules and this is due to the very low value of the dipole strength and consequently, of the oscillator strength f. The experimentally estimated value for the radiative lifetime of CQ was obtained on the basis of the Strickler-Berg formula [28]:

$$\frac{1}{\tau_f} = 2.88 \cdot 10^9 \, n^2 \; < \tilde{\nu}_0^{-3} >^{-1} \; \frac{g_{gs}}{g_{es}} \int \epsilon(\upsilon) \, d \ln(\nu)$$

where the integration is done over the entire absorption band of the fluorophore, n is the refracive index of the solvent, ν_0 is the wavenumber corresponding to the absortion maximum, ε is the molar absorptivity of the fluorophore, g_{gs} and g_{es} are the degeneracies of the ground and excited states, respectively.

The quantity can be calculated as:

$$< \tilde{\nu}_0^{-3} >^{-1} = \frac{\int \nu^{-3} \, F(\nu) d\nu}{\int F(\nu) d\nu}$$

where F(ν) is the intensity of the fluorescence signal.

Table 2. PCM-B3LYP/6-311+G(2d,p) calculated parameters for the excited state of camphorquinone in acetonitrile

	Calculated	**Experimental**
μ_{10}^2 (a.u.)	0.0097	n.a.
f	0.0003	n.a.
λ_{abs} (nm)	446	469
λ_{em} (nm)	502	514
τ_r (ns)	6451	5133
Φ	n.a.	n.a.
τ_f (ns)	n.a.	n.a.
τ_{nr} (ns)	n.a.	n.a.
$\Delta\lambda_{Stokes}$ (nm)	56	45

3.3. Geometry of the ground and excited state

The experimental geometry of Camphorquinone has been retrieved from the The Cambridge Crystallographic Data Centre (CCDC) (Refcode: CAMPQU, CCDC number: 1120029) [29]. The molecule crystallizes in the I2 space group with the unit cell parameters: a = 12.081 Å, b = 6.731 Å, c = 23.43 Å, α = 90°, β = 96.25° and γ = 90°.

Experimental and calculated geometrical parameters (bond lengths and valence angles) of CQ are summarized in Table 3. Besides the parameters of the ground state (S0) in gas-phase and acetonitrile we included also the parameters of the first excited state of CQ. As easily can be observed, the geometrical parameters of the ground state geometry are well reproduced by calculations. The largest discrepancies between the experimental and computed data are noted for the C3-C7 bond length and the C3C2O12 bond angle. Such discrepancies can be attributed to the fact that the calculations were performed on a single molecule and such a model cannot capture the intermolecular interactions inherent in solid phase.

Table 3. Experimental and B3LYP/6-311+G(2d,p) calculated geometrical parameters of Camphorquinone

Geometrical parameter	Experimental	Calculated B3LYP/6-311+G(2d,p)		
	X-ray	S0 (gas-phase)	S0 (acetonitrile)	S1 (acetonitrile)
C1-C2	1.554	1.571	1.569	1.492
C2-C3	1.511	1.516	1.506	1.549
C3-C4	1.535	1.554	1.557	1.552
C4-C5	1.535	1.556	1.554	1.557
C5-C6	1.549	1.562	1.566	1.559
C6-C7	1.558	1.577	1.580	1.558
C3-C7	1.533	1.561	1.564	1.544
C7-C8	1.522	1.537	1.536	1.534
C7-C9	1.537	1.532	1.532	1.546
C6-C10	1.510	1.515	1.516	1.513
C6-C1	1.496	1.527	1.517	1.581
C1-O11	1.204	1.200	1.205	1.223
C2-O12	1.179	1.200	1.205	1.227
C1C2C3	102.9	103.6	103.9	104.4
C2C3C4	103.5	104.5	104.3	104.6
C3C4C5	103.1	130.4	103.5	102.7
C4C5C6	105.3	104.6	104.7	103.9
C5C6C1	103.6	103.3	103.0	103.0

Geometrical parameter	Experimental	Calculated B3LYP/6-311+G(2d,p)		
	X-ray	S0 (gas-phase)	S0 (acetonitrile)	S1 (acetonitrile)
C5C6C7	101.8	102.1	102.0	102.9
C5C6C10	115.9	115.1	115.1	115.9
C6C1C2	105.4	104.5	104.8	104.5
C6C7C8	113.4	113.3	113.3	115.0
C6C7C9	113.0	114.0	113.9	113.0
C6C1O11	130.4	129.2	130.1	126.8
C3C2O12	131.0	126.3	130.8	127.7

* bond lengths in Å; angles in degrees

We were also interested in the change of CQ's geometry as a result of electronic excitation. For this purpose, the geometry of CQ was optimized in acetonitrile in ground (S0) and the first excited state (S1). Fig. 7 shows the two superimposed optimized geometries.

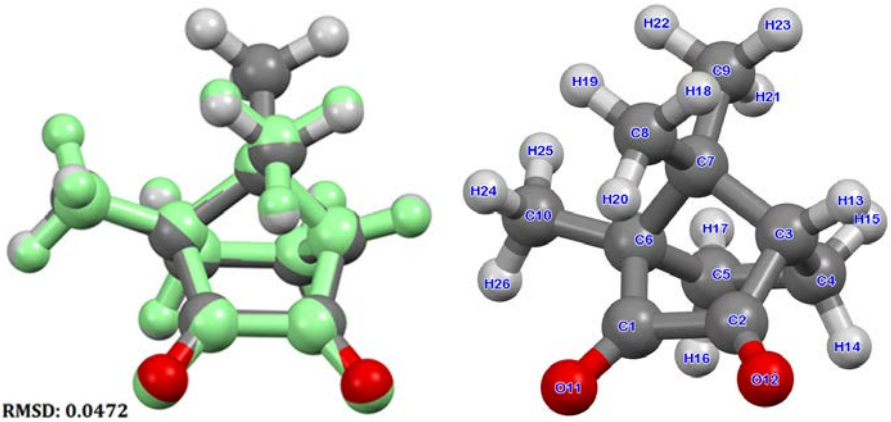

Fig. 7. left: Superimposed B3LYP/6-311+G(2d,p) of CQ in acetonitrile in ground state and excited state (light green); right: atom number scheme for CQ

According to theoretical results, the geometry of CQ is slightly distorted in the excited state, quantitatively, the average root mean square deviation (rmsd) between the backbone atoms being 0.0472 Å. The only geometrical parameters affected in an appreciable manner are the C1-C2 and C6-C1 bond lengths and the

bond angles involving the oxygen atoms (C6C1O11 and C3C2O12). Less deviations can be observed for the bonds involving the C7 atom (shortening of about 0.02 Å) and also, for the two C=O bonds which suffer a lengthening of cca. 0.02 Å. This distortion of the geometry in the S1 excited state is reflected in the relatively small Stokes shift observed for the calculated (and experimental) absorption and emission spectra of CQ (see Table 3.).

4. CONCLUSIONS

Absorption and emission spectra of the photoinitiator camphorquinone have been calculated at TD-DFT-B3LYP/6-31+G(2d,p) level of theory. The transition to the first excited state of Camphorquinone is an $n \rightarrow \pi^*$ transition and it was explained on the basis of the natural transition orbitals. The calculated electronic absorption energy (λ_{max} = 484 nm) was in excellent agreement with the available experimental data.

The vertical emission energy (514 nm), as well as the radiative fluorescence lifetime (6.45μs) has been computed for CQ. The most important structural parameters affected by the transition to the first excited state are those describing the two carbonyl groups.

ACKNOWLEDGMENTS

The research undertaken for this article was conducted using the Babeş-Bolyai University Research infrastructure financed by the Romanian Government through the project MADECIP (POSCEE COD SMIS CSNR 48801/1862)

REFERENCES

[1] R.L. Bowen, *J. Am. Dental Assoc.*, 66 (1963) 57-64; R.L Bowen, W.A. Marjenhoff, *Adv. Dent. Res*., 6 (1992) 44-49.

[2] J.F. Glenn, Composition and properties of unfilled and composite restorative materials. In: D.C. Smith, D.F. Williams, editors. *Biocompatability of dental materials*. Vol III. 10th ed. Boca Ration (FL): CRC Press; 1982. p. 98-125.

[3] L.J. Schneider, L.A. Cavalcante, S.A. Prahl, C.S. Pfeifer, J.L. Ferracane, *Dent. Mat*., 28 (2012) 392-397.

[4] J.G. Leprince, M. Hadis, A.C. Shortall, J.L. Ferracane, J. Devaux, G. Leloup et al., *Dent. Mat.*, 27 (2011) 157-164.
[5] G. Longhi, E. Castiglioni, S. Abbate, F. Lebon, D.A. Lightner, *Chirality*, 25 (2013) 589-599.
[6] Z. Okulus, T. Buchwald, M. Szybowicz, A. Voelkel, *Mat. Chem. Phys*. 145 (2014) 304-312.
[7] M.R. Casida, C. Jamorski, K.C. Casida, D.R. Salahub, *J. Chem. Phys.* 108 (1988) 4439-4449.
[8] Gaussian 09, Revision E.01, M.J. Frisch, G.W. Trucks, H.B. Schlegel, G.E. Scuseria, M.A. Robb, J.R. Cheeseman, G. Scalmani, V. Barone, B. Mennucci, G.A. Petersson, H. Nakatsuji, M. Caricato, X. Li, H.P. Hratchian, A.F. Izmaylov, J. Bloino, G. Zheng, J.L. Sonnenberg, M. Hada, M. Ehara, K. Toyota, R. Fukuda, J. Hasegawa, M. Ishida, T. Nakajima, Y. Honda, O. Kitao, H. Nakai, T. Vreven, J.A. Montgomery, Jr., J.E. Peralta, F. Ogliaro, M. Bearpark, J.J. Heyd, E. Brothers, K.N. Kudin, V.N. Staroverov, R. Kobayashi, J. Normand, K. Raghavachari, A. Rendell, J.C. Burant, S.S. Iyengar, J. Tomasi, M. Cossi, N. Rega, J.M. Millam, M. Klene, J.E. Knox, J.B. Cross, V. Bakken, C. Adamo, J. Jaramillo, R. Gomperts, R.E. Stratmann, O. Yazyev, A.J. Austin, R. Cammi, C. Pomelli, J.W. Ochterski, R.L. Martin, K. Morokuma, V.G. Zakrzewski, G.A. Voth, P. Salvador, J.J. Dannenberg, S. Dapprich, A.D. Daniels, Ö. Farkas, J.B. Foresman, J.V. Ortiz, J. Cioslowski, and D.J. Fox, Gaussian, Inc., Wallingford CT, 2009.
[9] A.D. Becke, *J. Chem. Phys*. 1993, 98, 5648.
[10] C. Lee, W. Yang, R.G. Parr, *Phys. Rev. B*, 37 (1988) 785.
[11] S. H. Vosko, L. Wilk, M. Nusair, *Can. J. Phys.* 1980, 58, 1200.
[12] P.J. Stephens, F.J. Devlin, C.F. Chabalowski, M.J. Frisch, *J. Phys. Chem*. 98 (1994) 11623-11627.
[13] R.L. Martin, *J. Chem. Phys*. 118 (2003) 4775-4777.
[14] S. Marković and J. Tošović, *J. Phys. Chem. A* 119 (2015) 9352-9362.
[15] J. Tomasi, B. Mennucci and R. Cammi, *Chem. Rev.* 105 (2005) 2999-3093.
[16] GaussView, Version 5, Roy Dennington, Todd Keith, and John Millam, Semichem Inc., Shawnee Mission, KS, 2009.
[17] C.F. Macrae, P.R. Edgington, P. McCabe, E. Pidcock, G.P. Shields, J. *Appl. Crystalogr.* 39 (2006) 453-457.
[18] T. Corrales, F. Catalina, C. Peinado, N.S. Allen, *J. Photochem. Photobiol. A: Chemistry,* 159 (2003) 103–114.
[19] E. Andrzejewska, L.-A. Linden, J.F. Rabek, Macromol. *Chem. Phys*. 199 (1998) 441.
[20] M.G. Neumann, W,G. Miranda Jr, C.C. Schmitt, F.A. Rueggeberg, I.C. Correa, *J. Dent.* 33 (2005) 525-532.
[21] D.C.R.S. de Oliveira, M.G. Rocha, A. Gatti, A.B. Correr, J.L. Ferracane, M.A.C. Sinhoreti, *J. Dent*. 43 (2015) 1565–1572.
[22] K. Ikemura, T. Endo, *Dent. Mat. J.* 29 (2010) 481–501.
[23] M.A.L. Marques, E. K.U. Gross, in: *Time dependent density functional theory*, eds. C. Fiolhais, F. Nogueira, M. Marques, p. 144–184, Springer-Verlag, Berlin 2003.
[24] J.B. Foresman and Æ. Frisch, *Exploring Chemistry with Electronic Structure Methods* (third edition), Gaussian Inc., 2015, Wallingford, CT USA.

[25] X. Zheng, Q. Peng, J. Lin, Y. Wang, J. Zhou, Y. Jiao, Y. Bai, Y. Huang, F. Li, X. Liu, X. Pua and Z. Lu, *J. Mater. Chem. C 3* (2015) 6970-6978.
[26] [Lou02] B. Lounis, M. Onil, *Rep Prog. Phys*., 68, (2005) 1129-1179.
[27] M. Savarese, A. Aliberti, D. De Santo, E. Battista, F. Causa, P. A. Netti and N. Rega, *J. Phys. Chem. A,* 116 (2012) 7491-7497.
[28] S. J. Strickler, R. A. Berg, *J. Chem. Phys.,* 37 (1962) 814-822.
[29] Cambridge Crystallographic Data Centre (CCDC) (Refcode: CAMPQU, CCDC number: 1120029). (accessed: 05.02.2017)